INTERNATIONAL JOURNAL OF CLIMATOLOGY
*Int. J. Climatol.* **33**: 2002–2007 (2013)
Published online 15 August 2012 in Wiley Online Library
(wileyonlinelibrary.com) DOI: 10.1002/joc.3568

RMetS
Royal Meteorological Society

# Seasonal and regional differences in the rainfall and intensity of isolated convection over South America

Thomas M. Rickenbach,[a]* Rosana Nieto-Ferreira,[a] Richard P. Barnhill[a,b] and Stephen W. Nesbitt[c]

[a] *Department of Geography, East Carolina University, Greenville, NC, USA*
[b] *Current affiliation: Earth Resources Technology, Inc., Silver Spring, MD, USA*
[c] *Department of Atmospheric Sciences, University of Illinois, Urbana-Champaign, Urbana, IL, USA*

**ABSTRACT:** Isolated precipitating convection, though a minor contributor to total rainfall in the tropics, is important to regional and seasonal climate variability because its diabatic heating structure is characteristic of the convectively inactive phase of tropical interseasonal oscillations. This study extends a previous analysis of mesoscale convective system (MCS) variability in the South America monsoon system to examine regional differences in the annual cycle of the rainfall and vertical structure of isolated convection over the 10 year period of 1998–2007. The goal is to document the annual variation of shallow and deep isolated convection in order to provide a more complete picture of monsoon onset across South America. Over the 10 year period of 1998–2007, the average rain contribution from isolated convection (compared to MCSs) ranged from 1 to 8% of the total rainfall in the four regions depending on the season. The contribution of rainfall by isolated convection was on the high end of that range during the pre-monsoon months of June to August in the tropical regions. Of the isolated convection rainfall, 4–9% was attributable to shallow 'warm rain', with the largest fraction after monsoon onset (December to February) in the coastal Mouth of Amazon region. Mean annual time series of conditional rainfall, lightning activity, 85 GHz ice-scattering signature, and radar echo depth for isolated convective features all suggested that an oceanic regime strongly influences isolated convection at the Mouth of Amazon region in northeastern Brazil. In the interior tropical regions, there was a clear pre-monsoon (August to September) maximum in the vertical intensity of deep isolated convection as indicated by lightning, ice scattering, and radar echo depth. Copyright © 2012 Royal Meteorological Society

KEY WORDS monsoon; convection; South America

*Received 3 January 2012; Revised 30 May 2012; Accepted 1 July 2012*

## 1. Introduction

Tropical cumulonimbus clouds enable the vertical energy transport that drives the general circulation of the atmosphere (Riehl and Malkus, 1958; Zipser *et al*., 2006). The precipitating 'hot towers' described in those papers (a reference to the latent heat energy released in cumulonimbus clouds) occur as isolated convective cells and as embedded convection within mesoscale convective systems (MCSs). Although isolated convection has been shown to be the most common mode of rainfall delivery from tropical ocean and land regions (Cheng and Houze, 1979; Keenan and Carbone, 1992; Rickenbach and Rutledge, 1998), MCSs dominate rainfall totals across the global tropics (Nesbitt *et al*., 2006) and over the major tropical continents. In tropical South America, Nesbitt *et al*. (2006) concluded from 3 years of Tropical Rainfall Measuring Mission (TRMM) satellite data that 60–90% of South American rainfall was produced by MCSs. This fraction was lower in the northeast and higher in the subtropical south, where the subgroup of large MCSs known as mesoscale convective complexes is common (Velasco and Fritsch, 1987; Durkee *et al*., 2009).

The fact that isolated convection is secondary to MCSs in the overall tropical rainfall budget does not diminish the importance of isolated convection to the energetics of the general circulation, particularly on a regional and seasonal scale. In the equatorial West Pacific Ocean, for example, isolated convection becomes the dominant rain producer during convectively suppressed phases of the Madden–Julian Oscillation (MJO) (Johnson *et al*., 1999). The vertical latent heat distribution in that situation contrasts fundamentally with the active MJO phase where diabatic heating is mainly accomplished by MCSs, leading to quite different impacts on the energetics of the ascending branch of the Hadley Cell in that region from month to month (Ling and Zhang, 2011). These studies lead to the conclusion that even though isolated convection is a minor contributor to total

* Correspondence to: T. M. Rickenbach, Department of Geography, East Carolina University, A-227 Brewster Bldg., Greenville, NC 27858-4353, USA. E-mail: rickenbacht@ecu.edu

tropical rainfall, its diabatic heating structure dominates during the convectively inactive phase of interseasonal oscillations, and during the rainfall minimum in the annual cycle. This variability is important to understand regional transitions of convective regimes associated with the MJO and with the seasonal cycle (Hendon and Salby, 1994; Carvalho *et al*., 2002).

Tropical and subtropical South America, one of the main global source regions of energy transport out of the tropics, has a complex monsoon climate (Kousky, 1988; Liebmann *et al*., 1999) that is strongly influenced by regional differences in dynamic and thermodynamic forcing of precipitation (Li and Fu, 2004). Nieto-Ferreira and Rickenbach (2011) described a conceptual model of South America monsoon onset that emphasized distinct regional onset mechanisms as a way to better understand the annual cycle of precipitation. These include the rapid establishment of the South American Convergence Zone related to a shift in the structure and propagation of cold fronts (Nieto-Ferreira *et al*., 2011), and the delayed onset of precipitation in northeastern Brazil due to the slow seasonal migration of the Atlantic Ocean intertropical convergence zone (Nieto-Ferreira and Rickenbach, 2011). The vertical intensity and rainfall amount of MCSs before *versus* after monsoon onset were found by Rickenbach *et al*. (2011) to be inversely related, with rainier and vertically weaker (less ice aloft ostensibly due to weaker updrafts) MCSs following onset across the entire monsoon region. They found that seasonal maxima in surface sensible and latent heat fluxes energized the more intense pre-monsoon MCSs in the transition to onset.

This study extends the Rickenbach *et al*. (2011) analysis of MCS variability in the South America monsoon system to examine regional differences in the annual cycle of isolated convection rainfall and vertical structure over the 10 year period of 1998–2007. The goal is to document the annual variation of shallow and deep isolated convection in order to provide a more complete picture of monsoon onset across South America. Section 2 describes the TRMM data set, Section 3 presents the seasonal contribution to total rainfall from shallow and deep isolated convection, Section 4 examines the annual cycle of isolated convection intensity, and Section 5 offers conclusions.

## 2. Data and methods

Nieto-Ferreira and Rickenbach (2011) studied the regional variability of the annual cycle of precipitation in South America. Their rotated empirical orthogonal function (REOF) analysis of the Global Precipitation Climatology Project–Version 2 (GPCP-v2) precipitation data suggested four regions of distinct annual variability of precipitation in the SAMS region (Figure 1) which they defined as West-Central Amazon (Region I), Mouth of Amazon (Region II), SACZ (Region III), and South (Region IV). Rickenbach *et al*. (2011) examined the annual cycle of precipitation and structural characteristics of MCSs in these four regions using pentad-averaged data from the TRMM satellite Precipitation Feature Database (PFDB; Nesbitt *et al*., 2000, 2006).

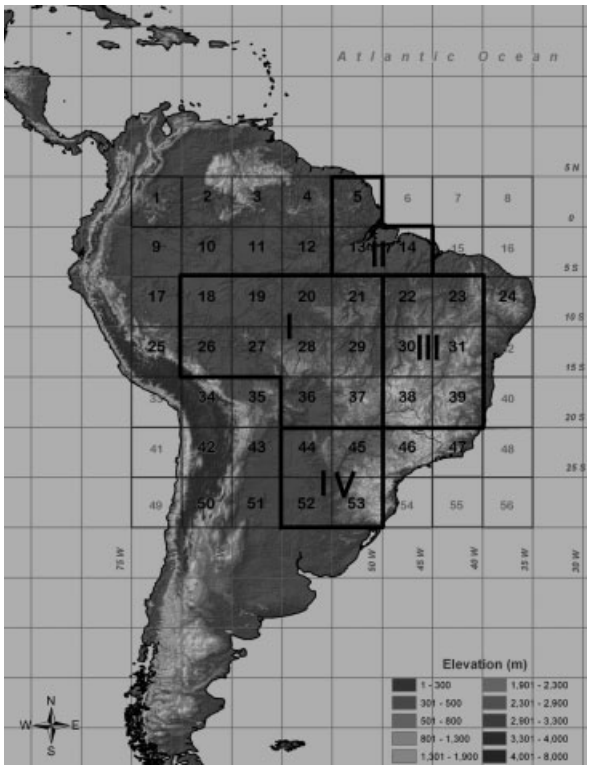


Figure 1. The SAMS domain divided into 5° × 5° land boxes (bold numbers) and analysis regions (Roman numerals) based on the first three REOFs of the GPCP-v2 pentad precipitation data. Regions are I – West-Central Amazon; II – Mouth of Amazon; III – SACZ; IV – South. Adapted from Rickenbach *et al*. (2011).

In this study, we extend the TRMM PFDB analysis of Rickenbach *et al*. (2011) to isolated precipitation features (PF). A TRMM PF represents either a contiguous portion of a MCS, or smaller groups of individual precipitating clouds, identified from the TRMM precipitation radar (PR) during each satellite overpass. Each PF is classified into one of three categories of organization and vertical structure following Nesbitt *et al*. (2000), using thresholds of TRMM PR reflectivity and TRMM Microwave Imager (TMI) polarization-corrected brightness temperature [polarization-corrected temperature (PCT)] at 85 GHz. The first category includes PFs that satisfy the size definition of a MCS (rain area $\geq$100 km in maximum elliptical dimension, following Houze, 1989) and contain an ice-scattering signature (minimum 85 GHz PCT $<$ 250 K) indicative of deep convective updrafts and strong convection. The second category contains smaller PFs with an ice-scattering signature that does not meet the rain area threshold of an MCS and is interpreted as deep isolated precipitating convective clouds or small groups of such clouds. The third category is defined as those smaller PFs without an ice-scattering signature, which includes isolated, shallow convection where warm rain processes

 

dominate precipitation formation. Each PF is identified instantaneously and is not tracked in time due to the TRMM satellite's inclined orbit giving at most two overpasses per day for a given location.

This paper focuses on the latter two categories: deep and shallow isolated convection. Rickenbach *et al*. (2011) described various PF metrics indicating the precipitation structure and intensity of convective systems. In this study, volumetric rainfall derived from the TRMM PR is used to determine the relative importance of shallow convection, deep convection, and MCSs to the seasonal (3 month mean) rainfall averaged over the 10 year period of 1998–2007. We then examine the mean annual cycle of conditional rain rate (rainfall divided by raining area, a measure of the rain intensity of the PF), lightning activity from the TRMM Lightning Imaging Sensor, feature depth measured by the vertical height of the 20 dBZ isosurface from the TRMM PR, and the minimum 85 GHz PCT as measured by the TMI. The latter three metrics are surrogates of the vertical intensity of the features, and represent independently measured aspects of the cloud system using physically distinct remote sensing techniques.

The PF metrics described above were averaged over each of the 5° boxes for each pentad from 1998 through 2007, and then averaged over each of the four analysis regions shown in Figure 1. The 5 day averages were taken to ensure sufficient sampling for robust estimates of each parameter. The pentad data were used to construct time series and composite averages of the mean (1998–2007) annual cycle for each parameter. The annual cycle time series were smoothed with a seven-point central moving filter to reduce the higher frequency variations associated with the relatively short 10 year sampling period.

Rickenbach *et al*. (2011) presented the annual cycle of various thermodynamic fields for each of the four regions using the National Center for Environmental Prediction Reanalysis dataset (Kalnay *et al*., 1996). We will refer to key conclusions from that analysis in the interpretation of the present results.

## 3. Rainfall contribution from isolated convection

Shown in Figure 2 is the fraction of the total rainfall attributed to isolated convection in each subregion of the SAMS. Over the 10 year period of 1998–2007, the average rain contribution from isolated convection (compared to MCSs) ranged from 1 to 8% of the total rainfall in the four regions depending on the season. This implies that MCSs dominate the large-scale rain variability on the annual cycle time scale over South America, since these four regions account for the primary modes of annual cycle rain variation (Nieto-Ferreira and Rickenbach, 2011). This result is consistent with TRMM satellite climatologies of MCS and stratiform rain over tropical land and ocean regions (Schumacher and Houze, 2003; Nesbitt *et al*., 2006). However, the contribution of rainfall by isolated convection was much larger during the 'dry' season months of June to August in the West-Central Amazon, Mouth of Amazon, and SACZ regions (Figure 2, upper panel). Specifically, in the West-Central Amazon and the SACZ region, nearly 8 and 7%, respectively, of the 'dry' season rain was associated with isolated convection with values near 2–3% for the rest of the year. This seasonal difference was statistically significant to greater than the 95% confidence level. At the Mouth of Amazon region, while the isolated convection contribution to rainfall (4.5%) was also significantly larger (>95% confidence interval) during June to August, this maximum was not as large as in the West-Central Amazon and SACZ regions. This suggests that, in contrast with these regions, conditions favour MCS organization for the Mouth of Amazon region, for example, the sea breeze as hypothesized by Rickenbach *et al*. (2011) and as suggested by the diurnal evolution of cloud cover in that region shown by Negri *et al*. (2000) and Rickenbach (2004). During the pre-monsoon (September to November) and the post-onset (December to February) months, the Mouth of Amazon isolated convection rainfall contribution for both shallow and deep features was larger than for the other regions. In the subtropical South region, the isolated convection rainfall contribution was steady year round at about 1%, consistent with the well-known importance of large MCSs to the water budget of that region (Durkee *et al*., 2009).

Of the small fraction of rainfall associated with isolated convection (both shallow and deep), the lower panel of Figure 2 indicates that across all regions and seasons, 4–9% of the isolated convection rainfall was attributable to shallow features. The largest fraction of shallow rain (9%) occurred after monsoon onset (December to February) in the coastal Mouth of Amazon region, having increased from a minimum of 7.2% in June to August, likely associated with the influence of maritime air along the coast (Section 4). The seasonal change of shallow convection rainfall fraction in the SACZ region was out of phase with that of the Mouth of Amazon, with a maximum of 8.7% in June to August. The West-Central Amazon and the South had the smallest contribution to isolated convection rainfall by shallow features compared to the other regions, with minima in June to August of 5 and 4.2%, respectively.

## 4. Annual cycle of isolated convection intensity metrics

Given that there exist regional differences in the rainfall contribution from shallow and deep isolated convection, it is useful to examine the 1998–2007 mean annual cycle of the rainfall intensity in these two cloud populations, together with the lightning and vertical structure of deep isolated convection, to give a clearer understanding of these differences. Conditional rain rate (annual cycle shown in Figure 3 for both shallow and deep isolated features) is defined as the average rain rate over

 

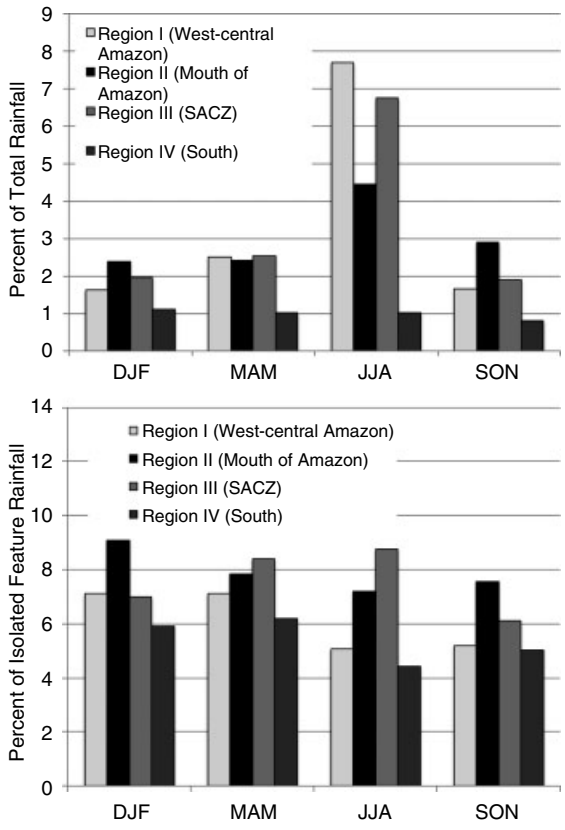


Figure 2. Upper panel: the fraction of the total 1998–2007 rainfall attributed to isolated convective features (both shallow and deep) for each region averaged for the indicated 3 month periods. Lower panel: the fraction of the isolated convective feature rainfall attributed to shallow convection for each region averaged for each 3 month period.

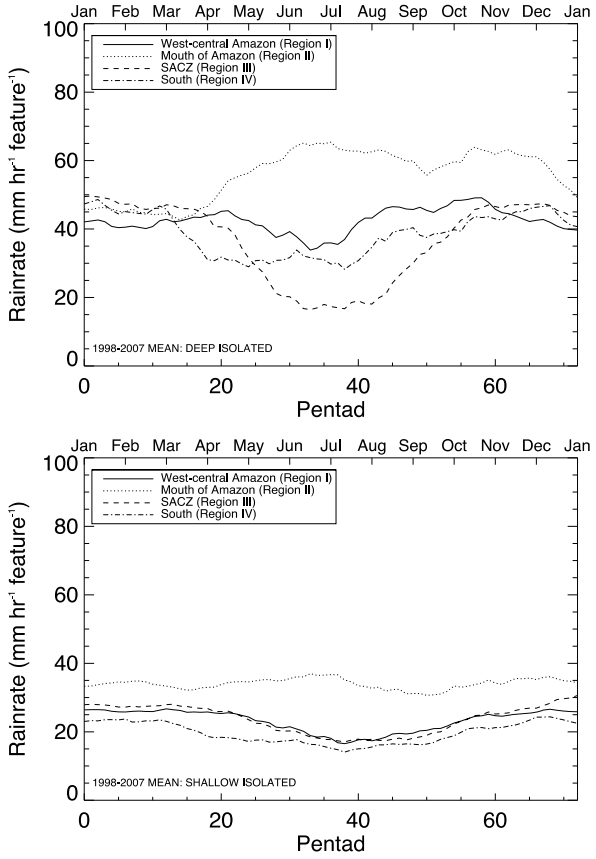


Figure 3. The 1998–2007 mean conditional rain rate (mm $hr^{-1}$ $feature^{-1}$) for isolated deep features (upper panel) and isolated shallow features (lower panel) in each of the four regions.

the raining area – a measure of the mean rain intensity of isolated features. For both feature types, the rain intensity drops by about 20–30% in the dry season months of June to August in all regions except the Mouth of Amazon. There, the deep isolated feature rain rate (Figure 3, upper panel) has a sustained maximum from June through December, about 30% greater than the wet season (December to March) maxima of the other three regions (statistically significant to greater than the 95% confidence level according to a Student's $t$-test). This result suggests that the relatively larger rain fraction associated with isolated convection in June to August (Figure 2) was caused by greater rain intensity.

In the case of shallow isolated features (Figure 3, lower panel), the Mouth of Amazon rain intensity is also higher by 30–50% compared to the other three regions (statistically significant to greater than the 95% confidence level), with essentially no annual cycle. The stronger rain intensity of shallow isolated features year round in the coastal Mouth of Amazon region is good evidence of an enhanced warm rain process associated with the maritime air mass in the prevailing easterly low-level wind of that region. The enhancement of Mouth of Amazon shallow convection thus suggests the influence of an oceanic regime. The other three regions show weaker rain intensity in the summer months, when latent heat flux and low-level moisture is diminished (Rickenbach *et al*., 2011).

Although the rain intensity for deep isolated convection is also larger in the coastal Mouth of Amazon region in the 'dry' season and pre-monsoon compared to the other regions, other metrics provide insight as to whether this difference is influenced more by warm or cold rain processes. The annual cycle of lightning activity for deep isolated convection (Figure 4) shows a pronounced seasonal cycle for all regions. The lightning flash rate (Figure 4, upper panel), which is the mean number of flashes from deep isolated convective features per unit time, reveals that the 'dry' season of June to August is clearly the most electrified period for isolated convection. The sole exception is the Mouth of Amazon where the flash rate maximum is lower by a factor of two or more, and occurs 1–2 months later (in September) compared to the other regions (statistically significant to greater than the 95% confidence level). This is consistent with the delayed monsoon onset in the Mouth of Amazon as well as the comparatively weaker, delayed maxima of sensible and latent heat in that region (Rickenbach *et al*., 2011). The annual cycle of the mean size of each deep isolated feature (not shown) appears very similar to the flash rate annual cycle, suggesting that the larger size of 'dry' season deep convective features in July in part leads to a higher flash rate over all regions.

 

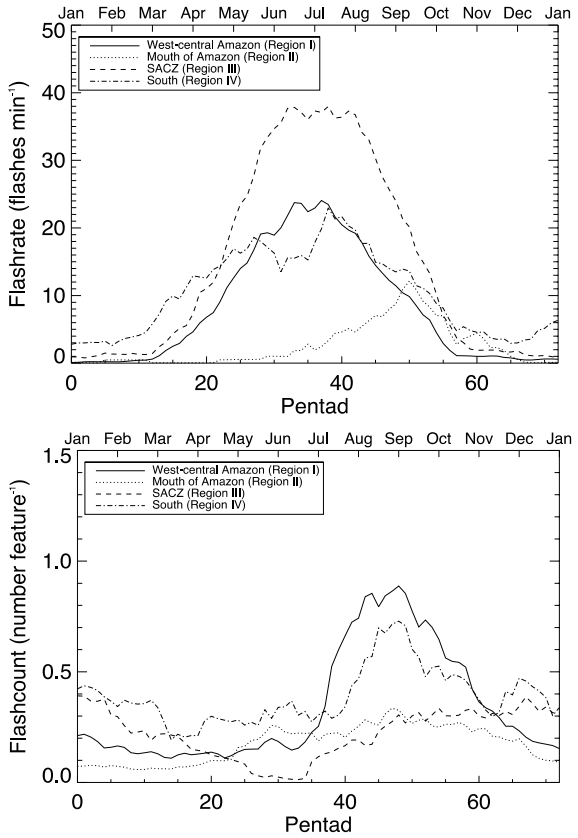


Figure 4. The 1998–2007 mean annual cycle of lightning flash rate and flash count for isolated deep features in each of the four regions. Upper panel shows the mean lightning flash rate (flashes $min^{-1}$) while lower panel shows the flash count per feature.

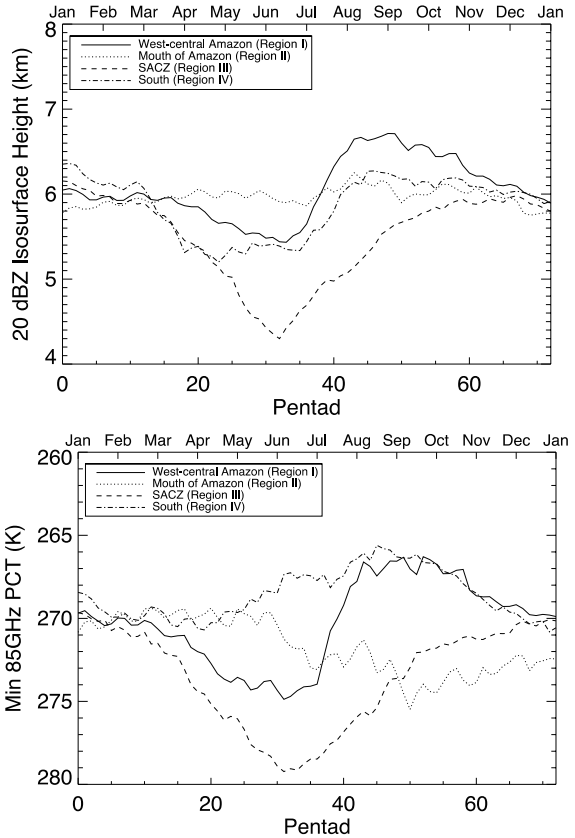


Figure 5. The 1998–2007 mean annual cycle of two metrics of vertical intensity for isolated deep features in each of the four regions. Upper panel shows the mean maximum height (km) of the 20 dBZ isosurface, while lower panel gives the mean minimum 85 GHz PCT (K) in an inverted vertical scale so that a stronger ice-scattering signature corresponds to lower temperature values farther up the vertical axis.

Considering the average number of flashes per feature (Figure 4, lower panel), a measure of the mean lightning intensity of isolated convection, lightning intensity reaches a clear annual maximum by August to September in West-Central Amazon, South, with a weak maximum at the Mouth of Amazon. The SACZ region, in contrast, had a sustained maximum in lightning intensity from August to December. Figure 4 suggests that although the peak flash rate (flashes $min^{-1}$) combining all deep isolated convective features occurs in July for the inland regions (September for Mouth of Amazon), the lightning flash count *per feature* (flashes per feature) is greatest in August to September for all regions. This reflects the superposition of the annual cycles of feature number and size such that there are relatively few but relatively large deep isolated features in August to September. There are essentially no lightning flashes associated with shallow isolated features, as expected due to the lack of ice microphysics in shallow clouds. The annual cycle of mean feature size for shallow isolated convection (not shown) is similar to that of deep isolated features, though about a factor of four smaller.

Other metrics of feature vertical intensity indicate stronger deep isolated convection in the pre-monsoon months of August to November, broadly consistent with the lightning results. The mean height of the 20 dBZ isosurface (Figure 5, upper panel), a measure of the vertical depth of the isolated features, showed a 15–20% increase during July leading to an August to September annual maximum in the West-Central Amazon and to a lesser extent the South, with a weaker and delayed maximum in the SACZ region. The Mouth of Amazon feature depth had very little annual variation, with slightly elevated values August to October. The minimum 85 GHz PCT (Figure 5, lower panel), an independent measure of vertical intensity via enhanced ice scattering, is broadly consistent with the PR-derived vertical depth. The pronounced July increase in minimum 85 GHz PCT in the West-Central Amazon corresponds exactly to the increase in feature depth and in lightning flashcount. The July to August maximum is likely controlled by a pronounced increase in sensible heat flux of similar phase (Rickenbach *et al.*, 2011) that corresponds to the 'dry' season increase of thermodynamic instability (Li and Fu, 2004). The more gradual and weaker increase in SACZ region feature depth from July to November is also seen in the minimum 85 GHz PCT. Interestingly, in the Mouth of Amazon region, the 85 GHz PCT actually increases (weakening ice-scattering signature) in the pre-monsoon months from July to October. This is consistent with the previous assertion that the high pre-monsoon conditional rain rates of deep isolated features in that coastal region

 

are tied to warm rain processes, as they are with the shallow features. Unique to the South, the 85 GHz PCT and the vertical depth indicate strengthening deep isolated convection from April to July in the lead-up to the 'dry' season. It was during April to July that the differences among all four regions in vertical depth and ice scattering were largest, statistically significant to greater than the 95% confidence level.

## 5. Conclusions

This paper extended the analysis of MCS variability in the South America monsoon system by Rickenbach *et al.* (2011) to examine regional differences in the annual cycle of isolated convection rainfall and vertical structure over the 10 year period of 1998–2007. The purpose was to document the annual variation of shallow and deep isolated convection in order to improve the understanding of the annual cycle of precipitation across South America.

Results indicated that isolated convection produces 1–8% of annual rainfall, with the highest contribution during the pre-monsoon months of June to August in the interior regions. Of the rainfall produced by isolated convection, 4–9% of the isolated convection rainfall was attributable to shallow features. Isolated convection in the Mouth of Amazon region in northeast Brazil reflected essentially an oceanic regime, with large year-round rain intensity despite weak lightning, ice scattering, and radar echo depth suggesting the dominance of warm rain processes in this coastal region. In the interior tropical regions, there is a clear pre-monsoon (August to September) maximum in the vertical intensity of deep isolated convection as indicated by lightning, ice scattering, and radar echo depth that coincide with an increase in sensible and latent heat fluxes (Rickenbach *et al.*, 2011).

For the tropical interior regions, the annual cycle of isolated convection vertical intensity is generally similar to that of MCSs (Rickenbach *et al.*, 2011). This suggests that the influence on MCS structure by the combination of pre-monsoon thermodynamic priming and aerosol loading, described by Rickenbach *et al.* (2011), similarly influences the structure of isolated convection. The exception was the Mouth of Amazon region, where the maritime influence on isolated convection was much clearer than for MCSs.

## Acknowledgements

This study was supported by a grant (NA07OAR 4310495) from the National Oceanic and Atmospheric Administration Climate and Global Change Program's Climate Prediction Program for the Americas (NOAA-CPPA).

## References

Carvalho LMV, Jones C, Silva Dias MAF. 2002. Intraseasonal large-scale circulations and mesoscale convective activity in tropical South America during the TRMM-LBA campaign. *Journal of Geophysical Research* **107**: D20, DOI: 10.1029/2001JD000745.

Cheng C, Houze RA. 1979. The distribution of convective and mesoscale precipitation in GATE radar echo patterns. *Monthly Weather Review* **107**: 1370–1381.

Durkee JD, Mote TL, Shepherd JM. 2009. The contribution of mesoscale convective complexes to rainfall across subtropical South America. *Journal of Climate* **22**: 4590–4605.

Hendon HH, Salby ML. 1994. The life cycle of the Madden-Julian oscillation. *Journal of the Atmospheric Sciences* **51**: 2225–2238.

Houze RA. 1989. Observed structure of mesoscale convective systems and implications for large-scale heating. *Quarterly Journal of the Royal Meteorological Society* **115**: 425–461.

Johnson RH, Rickenbach TM, Rutledge SA, Ciesielski PE, Schubert WH. 1999. Trimodal characteristics of tropical convection. *Journal of Climate* **12**: 2397–2418.

Kalnay E, Kanamitsu M, Kistler R, Collins W, Deaven D, Gandin L, Iredell M, Saha S, White G, Woollen J, Zhu Y, Chelliah M, Eblsuzaki W, Higgins W, Janowiak J, Mo KC, Ropelewski C, Wang J, Leetmaa A, Reynolds R, Jenne R, Joseph D. 1996. The NCEP/NCAR 40 year re-analysis project. *Bulletin of the American Meteorological Society* **77**: 437–472.

Keenan TD, Carbone R. 1992. A preliminary morphology of precipitation systems in tropical northern Australia. *Quarterly Journal of the Royal Meteorological Society* **118**: 283–326.

Kousky VE. 1988. Pentad outgoing longwave radiation climatology for the South American sector. *Revista Brasileira de Meteorologia* **3**: 217–231.

Li W, Fu R. 2004. Transition of the large-scale atmospheric and land surface conditions from the dry to the wet season over Amazonia as diagnosed by the ECMWF re-analysis. *Journal of Climate* **17**: 2637–2651.

Liebmann B, Kiladis GN, Marengo JA, Ambrizzi T, Glick JD. 1999. Submonthly convective variability over South America and the South Atlantic Convergence Zone. *Journal of Climate* **12**: 1877–1891.

Ling J, Zhang C. 2011. Structural evolution in heating profiles of the MJO in global reanalyses and TRMM retrievals. *Journal of Climate* **24**: 825–842.

Negri AJ, Anagnostou EN, Adler RF. 2000. A 10 yr climatology of Amazonian rainfall derived from passive microwave satellite observations. *Journal of Applied Meteorology* **39**: 42–56.

Nesbitt S, Cifelli R, Rutledge S. 2006. Storm morphology and rainfall characteristics of TRMM precipitation features. *Monthly Weather Review* **134**: 2702–2721.

Nesbitt SW, Zipser EJ, Cecil DJ. 2000. A census of precipitation features in the tropics using TRMM: radar, ice scattering, and lightning observations. *Journal of Climate* **13**: 4087–4106.

Nieto-Ferreira R, Rickenbach TM. 2011. Regionality of monsoon onset in South America: a three-stage conceptual model. *International Journal of Climatology* **31**: 1309–1321.

Nieto-Ferreira R, Rickenbach TM, Wright EA. 2011. The role of cold fronts in the onset of the monsoon season in the South Atlantic convergence zone. *Quarterly Journal of the Royal Meteorological Society* **137**: 908–922, DOI: 10.1002/qj.810.

Rickenbach TM. 2004. Nocturnal cloud systems and the diurnal variation of clouds and rainfall in southwestern Amazonia. *Monthly Weather Review* **132**: 1201–1219.

Rickenbach TM, Nieto-Ferreira R, Barnhill R, Nesbitt S. 2011. Regional contrast of mesoscale convective system structure prior to and during monsoon onset across South America. *Journal of Climate* **24**: 3753–3763.

Rickenbach TM, Rutledge SA. 1998. Convection in TOGA COARE: horizontal scale, morphology, and rainfall production. *Journal of the Atmospheric Sciences* **55**: 2715–2729.

Riehl H, Malkus JS. 1958. On the heat balance in the equatorial trough zone. *Geophysica* **6**: 503–538.

Schumacher C, Houze Jr. RA. 2003. Stratiform rain in the tropics as seen by the TRMM precipitation radar. *Journal of Climate* **16**: 1739–1756.

Velasco I, Fritsch M. 1987. Mesoscale convective complexes in South America. *Journal of Geophysical Research* **92**(D8): 9591–9613.

Zipser EJ, Cecil DJ, Liu C, Nesbitt SW, Yorty DP. 2006. Where are the most intense thunderstorms on Earth? *Bulletin of the American Meteorological Society* **87**: 1057–1071.

 